JOURNAL OF CATALYSIS 133, 309–324 (1992)

Physicochemical Properties of Ce-Containing Three-Way Catalysts and the Effect of Ce on Catalyst Activity

JOHN G. NUNAN,[1] HEINZ J. ROBOTA, MICHELLE J. COHN,* AND STEVEN A. BRADLEY*

*Allied–Signal Research and Technology; and *UOP Research Center, 50 East Algonquin Road, P.O. Box 5016, Des Plaines, Illinois 60017-5016*

Received May 17, 1991; revised July 30, 1991

The activity of Pt,Rh,Ce/γ-Al_2O_3 and Pt,Rh/CeO_2 catalysts has been studied in a full complement synthetic exhaust gas mixture consisting of H_2, CO, C_3H_6, C_3H_8, NO, O_2, N_2, CO_2, H_2O, and SO_2. Direct interaction between Pt and CeO_2 was shown to lead to large improvements in catalyst performance after activation of the catalyst in the synthetic exhaust gas. Catalyst activation was shown to be due to reduction of the noble metals and surface Ce and this state of the catalyst was found to be particularly effective for CO oxidation. The key component responsible for activation was shown to be H_2; even at the low H_2 level present in the exhaust gas ($\leq$0.26 vol%), reduction is shown to be very easy. The degree of Pt/Ce interaction, and thus activity, after catalyst activation could be controlled by varying the CeO_2 crystallite size. Decreasing the CeO_2 crystallite size led to greater Pt/Ce interaction as shown by TPR and STEM analysis and resulted in greater activity for both fresh and laboratory aged catalysts. Direct Pt/Ce interaction also led to a synergistic reduction of Pt and surface Ce which we found to qualitatively correlate with catalyst performance after activation.

INTRODUCTION

The effectiveness of CeO_2 in three-way-conversion catalysts is well established. However, the detailed role of CeO_2 in activity enhancement is still a subject of competing hypotheses. CeO_2 has been reported to act as an oxygen storage component (*1, 2*), to stabilize γ-Al_2O_3 (*3*), to promote water gas shift activity (*3, 4*), and to stabilize noble metal (NM) dispersion (*5*). CeO_2 has also been proposed to promote CO oxidation activity. Several mechanisms have been proposed to account for this selective promotion. These include retardation of CO inhibition during oxidation and a reduced activation energy for CO oxidation (*6, 7*). CeO_2 has also been proposed as a direct source of oxygen during CO oxidation (*7*), and reduced Ce has been linked to the formation of highly reactive O_2 radical anions (*8, 9*) that are very effective in oxidizing CO.

Several authors have also described synergistic interactions between NM and CeO_2. Some investigators have observed that reduction of Pt, Pd, and Rh is more facile when in contact with CeO_2 (*3, 10*). Also, coupling of NM and CeO_2 reduction was observed with reduction of both components at lower temperature than when they are not in contact. Yao and Yao (*10*) proposed that such synergism enhances oxygen storage by the catalyst.

Previous work has focused primarily on model reactions involving limited reactants using carefully activated catalysts. The present work addresses the performance of Pt,Rh,Ce/γ-Al_2O_3 catalysts in a full complement synthetic exhaust gas. Further, the catalysts studied were not initially activated by reduction before testing. We attempted to correlate some of the physicochemical properties of our catalysts with conversion performance in the synthetic exhaust gas. We describe the impact of exhaust gas composition and the degree of NM/Ce interac-

[1] To whom correspondence should be addressed.

0021-9517/92 $3.00

TABLE 1

Summary of Catalyst Compositions for Samples Used in Testing Having Varying CeO_2 Loadings and CeO_2 Crystallite Sizes

Sample #	Catalyst description	Metal content			CeO_2 crystallite size (111) (Å)
		Pt wt%	Rh wt%	Ce wt%	
1	Pt,Rh/γ-Al_2O_3	0.75	0.045	—	—
2	6% Ce/γ-Al_2O_3	—	—	5.52	61 ± 2
3	Pt,Rh, 6% Ce/γ-Al_2O_3	0.71	0.044	5.52	61 ± 2
4	Pt,Rh/γ-Al_2O_3	0.80	0.033	—	—
5	Pt,Rh, 6% Ce/γ-Al_2O_3	0.76	0.04	5.6	72 ± 2
6	Pt,Rh, 6% Ce/γ-Al_2O_3	0.76	0.041	5.67	113 ± 3
7	Pt,Rh, 6% Ce/γ-Al_2O_3	0.76	0.04	5.67	145 ± 4
8	Pt,Rh, 6% Ce/γ-Al_2O_3	0.79	0.041	5.70	213 ± 7
9	Pt,Rh, 6% Ce/γ-Al_2O_3	0.78	0.040	5.62	332 ± 16
10	Pt,Rh, 6% Ce/γ-Al_2O_3	0.79	0.048	4.99	~1000
11	Pt,Rh, 24% Ce/γ-Al_2O_3	0.34	0.066	24.1	65 ± 5
12	Pt,Rh, 25% Ce/γ-Al_2O_3	0.82	0.043	22.6	~1000
13	Pt,Rh, 25% Ce/γ-Al_2O_3	0.50	0.034	22.2	270 ± 5
14	Pt,Rh, 25% Ce/γ-Al_2O_3	0.77	0.042	21.5	130 ± 5
15	Pt,Rh, 25% Ce/γ-Al_2O_3	0.83	0.048	21.2	120 ± 5
16	Pr,Rh/γ-Al_2O_3	0.80	0.033	—	—

tion on the light-off activity of fresh, calcined catalysts and laboratory aged catalysts. Attempts were made to systematically vary the extent of NM/Ce interaction during catalyst preparation by using catalysts of varying CeO_2 loading and CeO_2 crystallite size. We show that direct interaction between CeO_2 and Pt leads to dramatic improvements in catalyst light-off activity after activation in the exhaust gas.

EXPERIMENTAL

A wide range of catalysts was prepared where the Ce loading, its method of introduction, and the CeO_2 crystallite size were varied. Table 1 describes the catalysts studied, including Ce loading, NM content, and the CeO_2 crystallite size (as measured by X-ray diffraction (XRD)). The NM and Ce contents were measured by inductively coupled plasma–atomic emission analysis. Different routes were followed to produce different CeO_2 sizes. Fresh catalysts having CeO_2 sizes in the range 60–110 Å were prepared by impregnation with various Ce salts and by using colloidal CeO_2. Samples with CeO_2 crystallite sizes of 110–350 Å were prepared by air calcining $Ce(NO_3)_3$ and $Ce(OAc)_3$ before milling the resulting CeO_2 together with γ-Al_2O_3. A highly sintered reagent CeO_2 powder was used to prepare samples 10 and 12. Samples 12–16 were laboratory aged before testing in 10% H_2O/90% air at 900°C for 4 hr and the CeO_2 crystallite sizes are given after aging. Following CeO_2 introduction, supports were sized to 425–850 μm with wire screens. Pt and Rh were introduced by impregnation with aqueous solutions of H_2PtCl_6 and $RhCl_3$; the catalysts were oven dried and finally calcined in air at 600°C for 6 hr.

Pure CeO_2 supports were prepared by precipitation of $Ce(NO_3)_3$ using $(NH_4)_2CO_3$ followed by filtration, drying, and calcination at 600°C for 6 hr. NMs were added as described.

Finished catalysts were evaluated in the full complement synthetic exhaust gas mixture shown in Table 2. It consisted of H_2, CO, C_3H_6, C_3H_8, NO, O_2, N_2, CO_2, H_2O,

TABLE 2

Exhaust Gas Composition Used for Catalyst Testing

Gas type mode	CO ppm	H_2 ppm	C_3H_8 ppm	C_3H_6 ppm	NO ppm	O_2 ppm	ER
Rich	8000	2667	267	167	1835	2790	2.02
Lean	3550	1183	118	167	1835	6500	0.50
Stoichiometric	5775	1925	193	167	1835	4645	~1.0

Note. Other components = 118,800 ppm CO_2, 20 ppm SO_2, 100,000 ppm H_2O. Balance = N_2.

and SO_2. Catalysts were tested in a tubular reactor using 1 g of catalyst and a flow rate of 5 liter/min. Catalysts could be exposed to rich (equivalence ratio (ER) 2.0), lean (ER = 0.5), or stoichiometric mixtures.

Different testing cycles were used with or without SO_2. The testing profile for tests without SO_2 is shown in Fig. 1. For this profile the catalysts were heated at 5°C/min in the stoichiometric mixture to 450°C (Rise-1), held at 450°C for 0.5 hr, cooled to 50°C in about 10 min, then reheated to 450°C in the stoichiometric mixture (Rise-2). Testing with SO_2 was similar except that the maximum temperature for Rise-1 and Rise-2 was 600°C, which was held for 1 hr. Higher temperatures were used for tests in the presence of SO_2 as this component is a strong poison for the present catalysts and temperatures of 600°C were required for complete conversion of the reactants and for maximum activation of the catalyst. During the hold and drop between Rise-1 and Rise-2, catalysts could be exposed to various combinations of rich, lean, and stoichiometric exhaust gas mixtures.

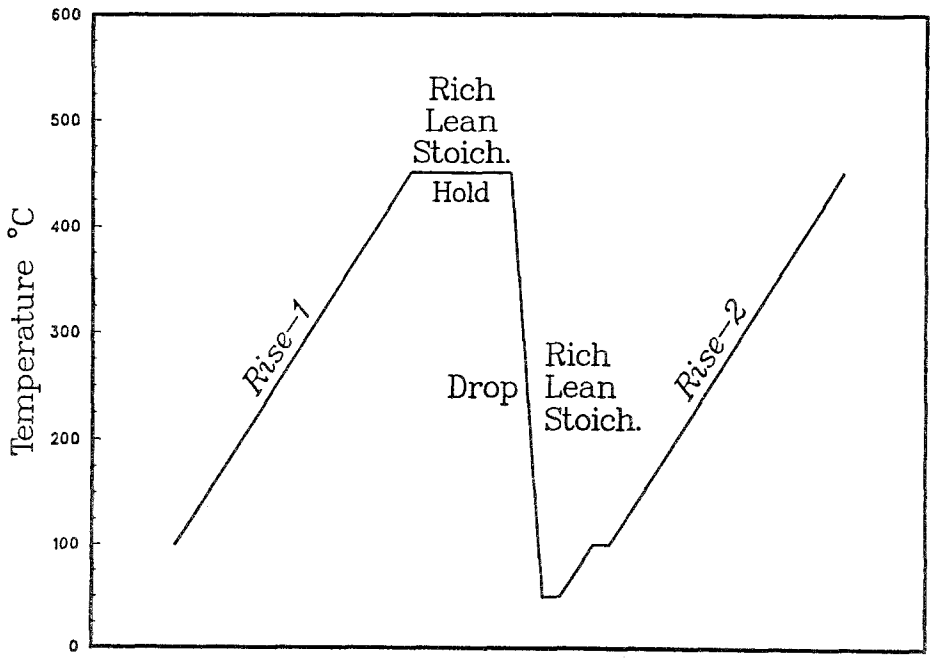

FIG. 1. Temperature profile used for catalyst testing in the absence of SO_2.

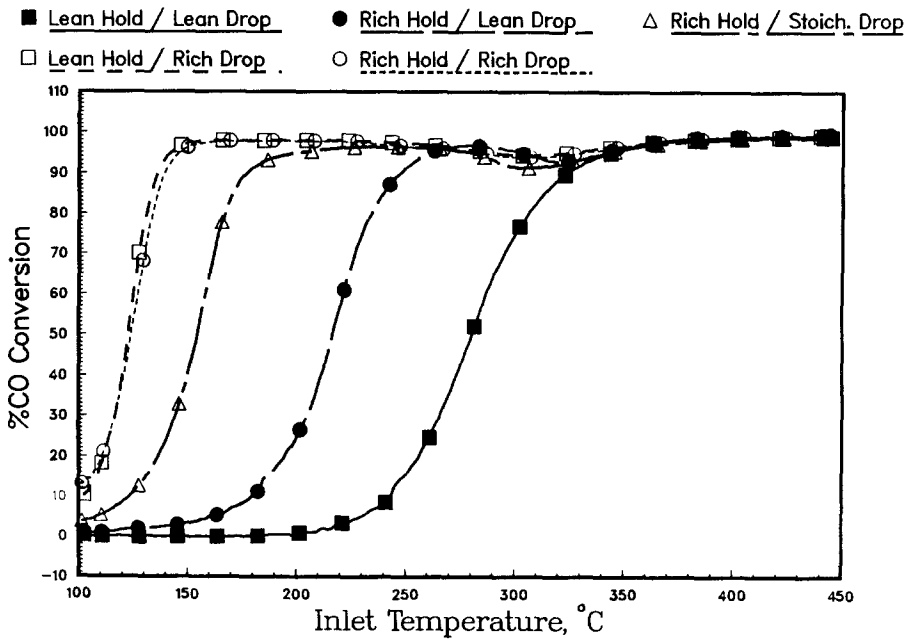

FIG. 2. Effect of various *in situ* conditionings in the non-SO_2 synthetic exhaust gas mixture on the Rise-2 light-off activity for CO. Catalyst = Pt,Rh, 24 wt% Ce/γ-Al_2O_3. Pt loading = 0.34 wt%; Rh loading = 0.06 wt%.

The catalysts were characterized using XRD, X-ray photoelectron spectroscopy (XPS), scanning transmission electron microscopy (STEM), and temperature programmed reduction (TPR). Both TPR and XPS measurements were carried out on fresh samples and on samples that had been treated in the synthetic exhaust gas. Samples analyzed after pretreatments in the exhaust gas were removed from the reactor in N_2 (O_2 content $\approx$ 50 ppm) and the TPR was carried out without further pretreatment.

RESULTS

Testing of the Pt,Rh,Ce/γ-Al_2O_3 catalysts showed that they were subject to large activity changes following exposure to exhaust gas, especially when Pt,Rh, and Ce were all present. Some activity change was expected as the catalysts were not initially activated by reduction. However, the considerable variation in catalyst activity related to exhaust gas composition was unexpected. The nature of the activation and the experimental factors that control its onset were studied in detail over sample 11. This was done by exposing the catalyst to varying combinations of rich, lean, and stoichiometric gas after Rise-1 and studying the effect on the Rise-2 light-off. The effect on CO oxidation during Rise-2 light-off is shown in Fig. 2. It is evident that Rise-2 light-off activity is very sensitive to the exhaust gas composition seen by the catalyst prior to Rise-2. The lowest Rise-2 activity occurs after a lean hold/lean drop whereas the highest activity occurs after a rich hold/rich drop and after a lean hold/rich drop. Clearly, catalyst activation is associated with exposure to rich exhaust gas. Activation of the catalyst after a lean hold by the rich drop further showed that the exhaust gas composition to which the catalyst is exposed during the drop is critical in the activation. Further, a rich hold followed by a drop in N_2 resulted in activation equivalent to a rich hold/rich drop. Thus, the rich drop can either activate the catalyst or maintain the catalyst in the acti-

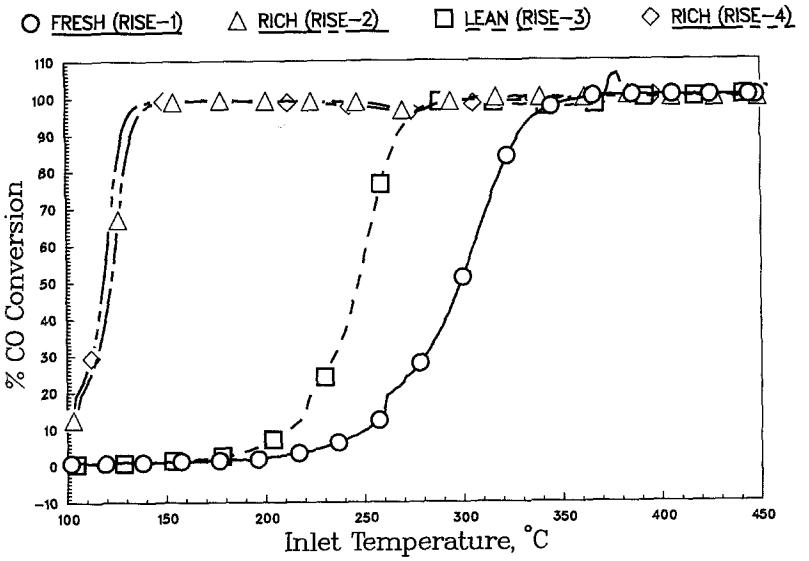

FIG. 3. Comparison of fresh light-off activity (Rise-1) for CO conversion and the activity after rich (Rise-2), lean (Rise-3), and rich (Rise-4) preconditioning. Catalyst = Pt,Rh, 24 wt% Ce/γ-Al_2O_3. Pt loading = 0.34 wt%; Rh loading = 0.06 wt%.

vated state. The drop between Rise-1 and Rise-2 takes about 10 min, indicating that activation is accomplished rapidly. It was also found that the activation/deactivation phenomenon was highly reversible. This is shown in Fig. 3 where the light-off activity for CO over a fresh catalyst, followed by subsequent rich, lean, and rich treatments at 450°C for 0.5 hr, is shown. It is clear that lean conditioning after rich conditioning results in loss of activity which can be recovered by a subsequent rich treatment.

The gas components contributing to activation were determined by removing various components one at a time from the rich drop, followed by another ramp in the full complement gas. Removal of CO, hydrocarbon (HC), and O_2 had no effect on catalyst activation. However, subsequent removal of H_2 was found to have a dramatic effect. Figure 4 compares Rise-2 light-off for CO oxidation with CO_2, NO, H_2O, and H_2 present during the drop to the case where only CO_2, NO, and H_2O remain. Clearly, removal of H_2 leads to complete loss of activation. Similar changes in catalyst performance were observed for HC and NO conversion. Apparently, catalyst activity can be dramatically altered by a low concentration of H_2 (0.26 vol%) in a relatively short time period.

The effect of various treatments on Rise-2 activity was also studied in the presence of SO_2 using the testing profile previously described. In Fig. 5 is shown the effect on the Rise-2 light-off activity for CO of a rich hold/rich drop as compared to a lean hold/lean drop. It is evident that the rich treatment leads to large activation of the catalyst, as observed previously for SO_2-free conditions. However, the lean hold/lean drop now leads to large deactivation of the catalyst. The difference in the CO light-off temperature between the lean and rich treated samples is nearly 250°C. Similar effects where also observed on the HC and NO light-off activity of the catalyst as a function of conditioning. Thus, catalyst performance is even more sensitive to conditioning where SO_2 is present than when it is absent. It was also found that the activation/deactivation phenomenon was highly reversible with

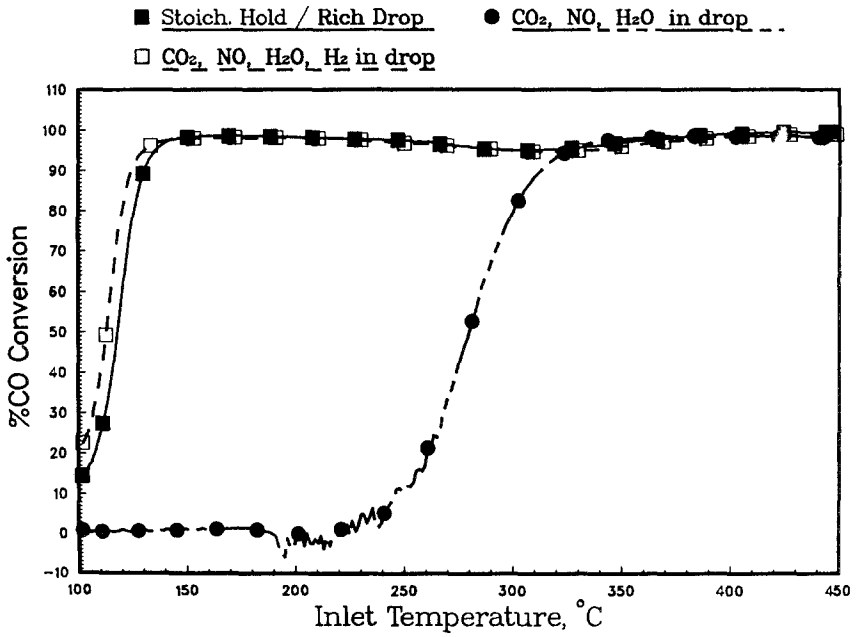

FIG. 4. Effect of removing H_2 from the rich exhaust gas mixture during the drop immediately before the Rise-2 on the subsequent CO light-off activity. Catalyst = Pt,Rh, 24 wt% Ce/γ-Al_2O_3. Pt loading = 0.34 wt%; Rh loading = 0.06 wt%.

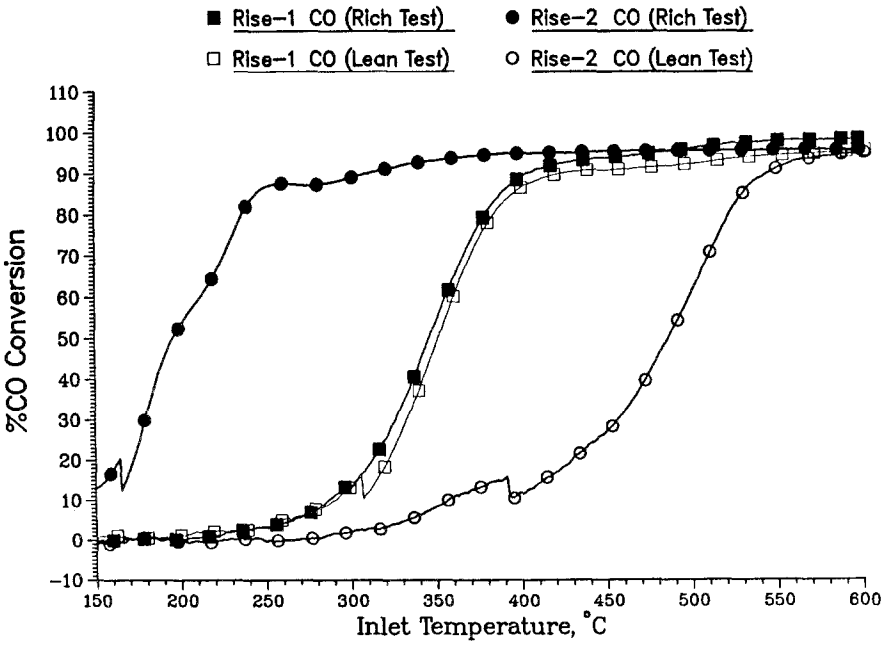

FIG. 5. Effect of a rich hold and drop as compared to a lean hold and drop on the CO light-off activity. Catalyst = Pt,Rh, 24 wt% Ce/γ-Al_2O_3. Pt loading = 0.34 wt%; Rh loading = 0.06 wt%.

TABLE 3

Comparison of Fresh Light-off Activity (Rise-1) for CO, HC, and NO Conversion and the Activity after Rich (Rise-2), Lean (Rise-3), and Rich (Rise-4) Preconditioning

Conditioning	Temp. at 25% conv.			Temp. at 50% conv.		
	CO	HC	NO	CO	HC	NO
Fresh (Rise-1)	310	375	502	345	452	570
Rich (Rise-2)	177	245	242	190	251	251
Lean (Rise-3)	302	325	310	320	330	325
Rich (Rise-4)	185	250	245	210	255	252

Note. Catalyst = Pt,Rh, 24 wt% Ce/γ-Al_2O_3. Pt loading = 0.34 wt%; Rh loading = 0.06 wt%.

SO_2 present. The results are summarized in Table 3 where the temperatures for 25 and 50% conversion for CO, HC, and NO are summarized for the fresh light-off activity and after subsequent rich, lean, and rich conditioning, respectively. It is noted that lean conditioning following rich conditioning does not lead to the same degree of deactivation as observed for lean conditioning of the fresh catalyst.

The effect of CeO_2 crystallite size on catalyst performance was studied both with and without SO_2. Fresh catalysts 4–10 were tested without SO_2. Rise-1 and Rise-2 activities are compared in Figs. 6 and 7. The catalysts were exposed to a stoichiometric mixture after Rise-1. Relative activities are compared using the temperatures at 25% CO, HC, and NO conversion plotted vs CeO_2 crystallite size. CeO_2 crystallite sizes shown were determined by XRD line broadening of the (111) reflection. As evident in

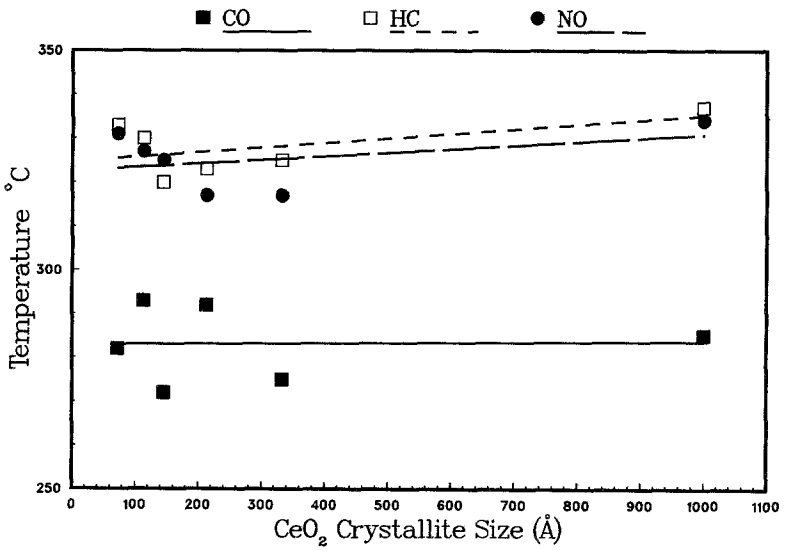

FIG. 6. Plot of CeO_2 crystallite size (111) as a function of the Rise-1 activity for CO, HC, and NO for testing in a stoichiometric exhaust gas mixture without SO_2. Activity is expressed as the temperature needed for 25% conversion. Catalyst = Pt,Rh, 6 wt% Ce/γ-Al_2O_3. Pt loading (nominal) = 0.77 wt%; Rh loading (nominal) = 0.04 wt%.

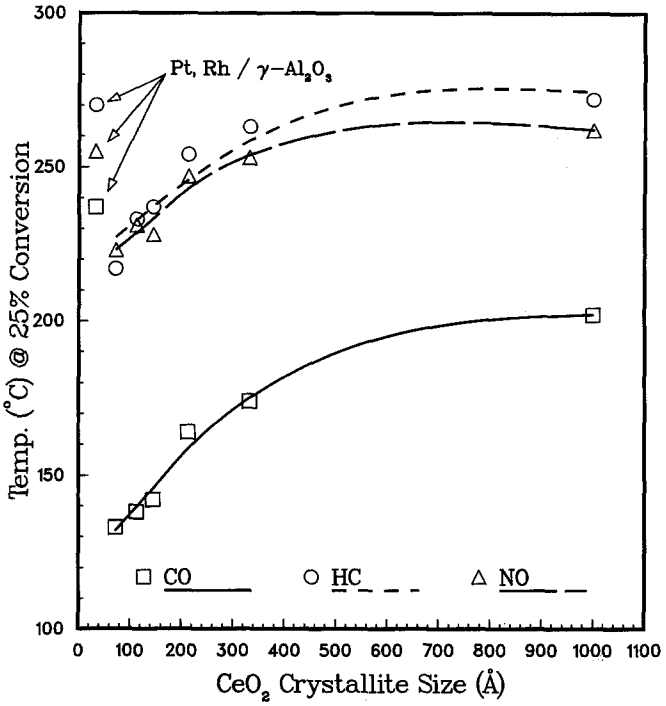

FIG. 7. Plot of CeO_2 crystallite size (111) as a function of Rise-2 light-off activity for CO, HC, and NO for testing in a stoichiometric exhaust gas mixture without SO_2. Activity is expressed as the temperature needed for 25% conversion. Catalyst = Pt,Rh, 6 wt% Ce/γ-Al_2O_3. Pt loading (nominal) = 0.77 wt%; Rh loading (nominal) = 0.04 wt%.

Fig. 6, CeO_2 size has no effect on Rise-1 activity. However, this is clearly not the case for Rise-2. Figure 7 reveals dramatic improvement in light-off activity for all three exhaust gas components with diminishing CeO_2 crystallite size, especially for sizes less than 250 Å. It is also observed that the activity of the $Pt,Rh/\gamma$-Al_2O_3 sample is lower than that for the Ce-containing samples. Further, a comparison of Figs. 6 and 7 shows that performance improvement is not the same for all components. The promotion of CO conversion ($\Delta T \approx 150$°C) is appreciably greater than that of HC ($\Delta T \approx 100$°C) or NO ($\Delta T \approx 100$°C) conversion. Since CeO_2 size has essentially no effect on Rise-1 activity, it is also clear that CeO_2 size is affecting the degree of catalyst activation.

Laboratory aged samples were tested with SO_2. Catalysts were exposed to stoichiometric exhaust during the hold and drop following Rise-1. Rise-2 light-off activities are summarized in Table 4. Also shown are the CeO_2 crystallite sizes after aging and testing. Clearly, large improvements in Rise-2 activity are observed for all three components with decreasing CeO_2 size. An approximately 80°C reduction in CO, HC, and NO 25% conversion temperature accompanies the reduction of CeO_2 size from 270 to 120 Å.

Several fresh samples with varying CeO_2 size were analyzed by scanning transmission electron microscopy (STEM). It was observed that a larger fraction of the Pt was associated with CeO_2 than expected based on the relative surface area exposed by CeO_2 compared with γ-Al_2O_3. Further, the fraction of Pt associated with CeO_2 increased with decreasing CeO_2 size. Thus, for maximum Pt/CeO_2 interaction, we need supports with the smallest CeO_2 size. This

TABLE 4

Rise-2 Light-off Activity for CO, HC, and NO over a Series of Aged Pt,Rh, 25 wt% Ce/γ-Al_2O_3 Samples Having Varying CeO_2 Crystallite Sizes (Activity Expressed as the Temperature for 25% Conversion)

Catalyst	CeO_2 crystallite size (Å) (111)	Temp. for 25% conv. (°C)		
		CO	HC	NO
Pt,Rh, 25 wt% Ce/γ-Al_2O_3	120 ± 5	300	315	295
Pt,Rh, 25 wt% Ce/γ-Al_2O_3	130 ± 5	310	330	307
Pt,Rh 25 wt% Ce/γ-Al_2O_3	270 ± 5	380	390	380
Pt,Rh, 25 wt% Ce/γ-Al_2O_3	≧1000	400	417	400
Pt,Rh/γ-Al_2O_3	—	425	440	425

Note. Pt loading (nominal) = 0.77 wt%; Rh loading (nominal) = 0.04 wt%.

observation suggests that the effect of CeO_2 crystallite size is related to increased Pt/Ce interaction. In order to test this hypothesis, Pt was supported separately on CeO_2 and γ-Al_2O_3. The temperatures required to achieve 25% conversion are reported in Table 5. Unlike the previous tests, these catalysts were exposed to the rich exhaust during the hold and drop following Rise-1. It is evident that Pt alone supported on pure CeO_2 undergoes large activations when exposed to the rich exhaust gas following Rise-1. It is further evident that the Rise-2 activities of the Pt/CeO_2 samples are much greater than those for the Pt/γ-Al_2O_3 samples. Thus, the results shown in Table 5 and Figs. 6 and 7 clearly demonstrate the beneficial effect of CeO_2 in promoting catalyst activation in stoichiometric or rich exhaust gas.

Since activation of the CeO_2 containing samples was clearly associated with exposure to H_2 in the exhaust gas, several fresh examples of the above catalysts were characterized using TPR. These included samples 1–3, 5, 8, and 10. The purpose of the analysis was to determine the effect of both CeO_2 introduction and CeO_2 crystallite size on catalyst reduction. Figure 8 shows the TPR spectra of the γ-Al_2O_3 support, Pt, Rh/γ-Al_2O_3, Ce/γ-Al_2O_3, and Pt,Rh,Ce/γ-Al_2O_3 (samples 1–3). Quantitative H_2 uptake values are tabulated in Table 6. The γ-Al_2O_3 substrate takes up some H_2 at about 700°C. This feature is present in Pt,Rh/γ-Al_2O_3 and Ce/γ-Al_2O_3 over a similar temperature range. One broad low temperature reduction, centered at 260°C, is assigned to reduction of Pt and Rh in the Pt,Rh/γ-Al_2O_3 catalyst. Since the Rh content of these samples is very low, distinct features of Rh reduction were not distinguishable. The 0.085 mmole of H_2 consumed is consistent with the amount required for complete Pt + Rh reduction (0.083 mmole). H_2 uptake by the

TABLE 5

Effect of Varying the Support Composition on the Rise-1 and Rise-2 Light-off Activities for CO, HC, and NO (Activity Expressed as the Temperature Needed for 25% Conversion)

Catalyst	SO_2	Temperature at 25% conversion					
		Rise-1			Rise-2		
		CO	HC	NO	CO	HC	NO
Pt/γ-Al_2O_3	No	282	365	360	245	342	340
Pt/CeO_2	No	355	450	>450	105	305	315
Pt/γ-Al_2O_3	Yes	417	425	440	427	442	460
Pt/CeO_2	Yes	387	430	560	160	272	282

Note. Testing was done in a stoichiometric exhaust gas mixture with a rich hold/rich drop between Rise-1 and Rise-2. Pt loading (nominal) = 0.6 wt%.

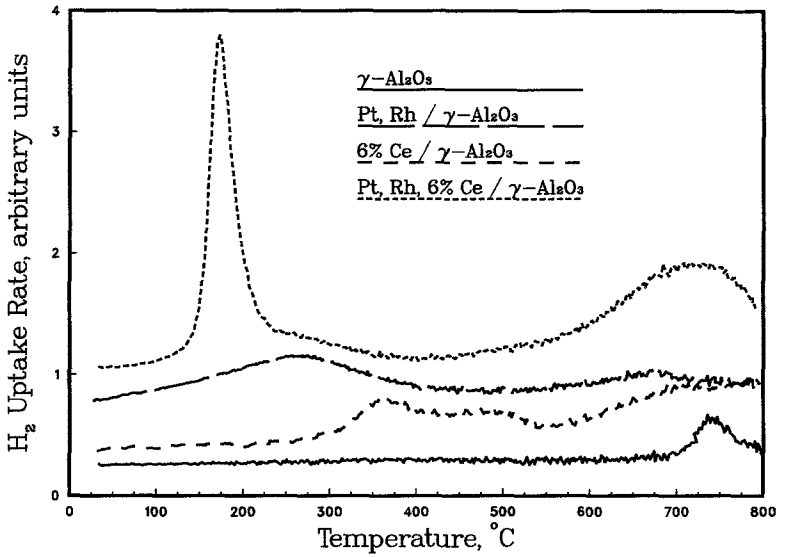

FIG. 8. Comparison of the TPR spectra for (a) γ-Al_2O_3; (b) Pt,Rh/γ-Al_2O_3; (c) 6 wt% Ce/γ-Al_2O_3; (d) Pt,Rh, 6 wt% Ce/γ-Al_2O_3. Pt loading (nominal) = 0.77 wt%; Rh loading (nominal) = 0.04 wt%.

Ce/γ-Al_2O_3 sample is shown in Fig. 8(c). Distinct peaks centered at 360 and 490°C and a broad feature above 600°C are observed. The low temperature peaks have been previously assigned to surface Ce reduction (*10, 11*) and the feature above 600°C is probably due to both H_2 uptake by γ-Al_2O_3 and some bulk Ce reduction. The TPR spectrum of Pt,Rh,Ce/γ-Al_2O_3 is shown in Fig. 8(d). The spectrum is clearly not a superposition of the previous two, but instead, has completely new features consisting of a sharp low temperature peak centered at 175°C, a shoulder at 280°C, and a broad peak centered at 720°C. The shoulder at 280°C is likely due to reduction of the Pt,Rh on the γ-Al_2O_3 component of the catalyst. We see no evidence for surface Ce reduction peaks below 500°C and the Pt,Rh/γ-Al_2O_3 peak is clearly attenuated, as shown by comparing H_2 uptakes in Table 6. Further, the H_2 uptake in the low temperature peak is greater than expected for exclusively Pt,Rh reduction. The absence of a distinct surface Ce reduction feature suggests that the extra reduction at low temperature is associated with surface Ce. Thus, this low temperature reduction feature appears to be a synergistic reduction of Pt,Rh + some surface Ce. Such a synergistic reduction in NM/Ce containing catalysts has been observed previously (*3, 10*). Again, we attribute the high temperature uptake to reduction of bulk Ce and uptake by γ-Al_2O_3.

The influence of CeO_2 crystallite size on catalyst reducibility was also examined. Results for samples 5, 8 and 10 are shown in

TABLE 6

Summary of the H_2 Uptake Values as Determined from TPR for (a) γ-Al_2O_3; Pt,Rh/γ-Al_2O_3; (b) 6 wt% Ce/γ-Al_2O_3; and (c) Pt,Rh, 6 wt% Ce/γ-Al_2O_3

Sample description	Temperature range °C	Temperature maximum °C	H_2 uptake mmole/g
γ-Al_2O_3 support	37–797	710	0.064
Pt,Rh/γ-Al_2O_3	29–481	260	0.085
	481–794	672	0.069
6 wt% Ce/γ-Al_2O_3	33–439	361	0.061
	439–560	490	0.034
	560–736	690	0.070
	736–795	795	0.090
Pt,Rh, 6 wt% Ce/γ-Al_2O_3	35–235	175	0.099
	235–407	280	0.030
	407–790	720	0.184

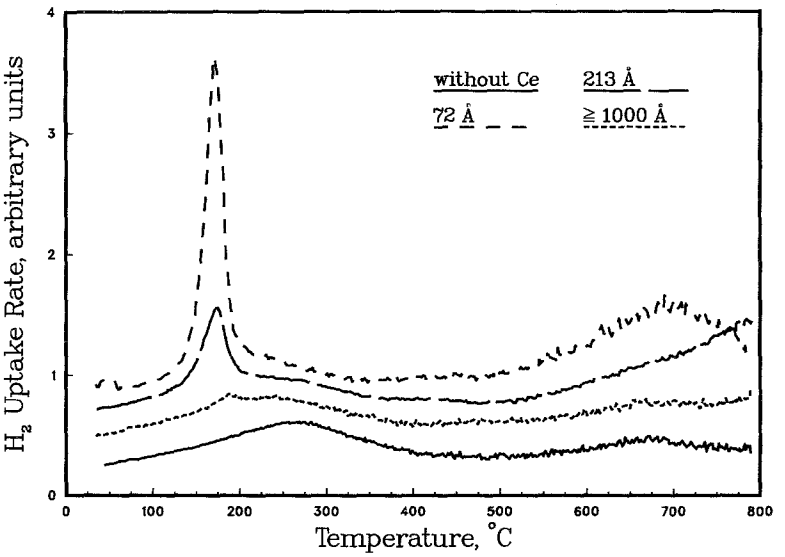

FIG. 9. Effect of CeO_2 introduction and the CeO_2 crystallite size (111) on the TPR spectra for a series of Pt,Rh, 6 wt% Ce/γ-Al_2O_3 samples. Pt loading (nominal) = 0.77 wt%; Rh loading (nominal) = 0.04 wt%.

Fig. 9. Sample 1 is also shown for comparison. Changing the CeO_2 crystallite size has a large impact on the TPR spectra, especially at lower temperatures. Decreasing the CeO_2 size leads to a systematic increase of the low temperature peak at 175°C, which has been assigned to the synergistic reduction of Pt,Rh + surface Ce. The appearance of this peak and its growth with decreasing CeO_2 size follow the previously observed trend of improved light-off for smaller CeO_2 size.

The effect of catalyst preconditioning on the TPR spectra was studied in detail for a Pt,Rh/CeO_2 sample. TPR was run on a fresh sample and after conditioning in model rich and lean exhaust at 450°C for 0.5 hr. Results are summarized in Fig. 10 and Table 7. Clearly, conditioning in rich or lean exhaust has a large impact on catalyst reduction. For the fresh sample we see a single sharp H_2 uptake at 180°C which is about 4.5 times greater than that needed for Pt,Rh reduction. This suggests that most of the H_2 uptake is associated with the CeO_2 support. There is no evidence for distinct surface Ce reduction between 300 and 500°C as reported by other authors (*3, 10, 11*). However, above 500°C, there is additional gradual H_2 uptake. The H_2 uptake in the temperature region between 500 and 650°C may be associated with some high temperature surface Ce reduction and the uptake above 700°C with bulk Ce reduction. In the lean and rich treated samples, H_2 uptake above 500°C is very similar to that of the fresh sample as seen by comparing the spectra in Fig. 10 with the H_2 uptake values in the temperature ranges 250–700°C and 700–800°C in Table 7. Lean conditioning results in a moderate decrease in low temperature reduction with a distinct shift to 100°C. In contrast, rich conditioning causes a net decrease in uptake centered at 80°C. Thus, under rich gas conditions, extensive catalyst reduction occurs. As for Pt,Rh, Ce/γ-Al_2O_3 samples, we see no evidence of separate Pt and Rh reduction, suggesting that reduction of both noble metals occurs under the low temperature peak.

Pt,Rh/CeO_2 and Pt,Rh,Ce/γ-Al_2O_3 samples were characterized using XPS after rich

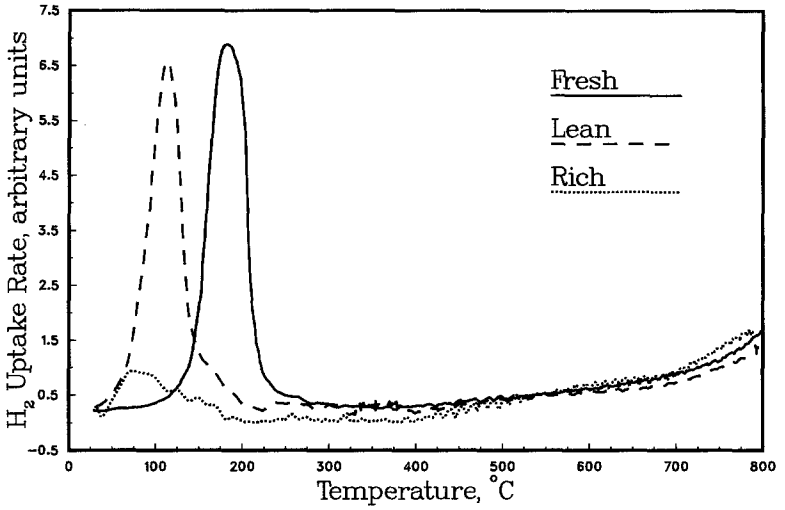

FIG. 10. Comparison of the TPR spectra for a Pt,Rh/CeO_2 sample before conditioning and after conditioning in the synthetic exhaust gas mixture under rich and lean conditions at 450°C for 0.5 hr. Pt loading = 0.6 wt%; Rh loading = 0.1 wt%.

and lean conditioning in the exhaust gas at 450°C for 0.5 hours. The samples were removed under N_2 and transferred to the XPS instrument. During the XPS experiment sample charging was compensated by using a low energy electron flood gun. The binding energies were then internally referenced to the O1*s* peak located at 528.84 eV. Some of the XPS peak intensities were very weak due to the low levels of NM present and only the peak positions for the more intense peaks are reported. The reported peak positions are accurate to ±0.2 eV. Peak positions and their assignments are summarized in Table 8. The lean conditioned Pt, Rh/CeO_2 sample has peaks located at 75.8 eV (Pt4$f_{5/2}$) and 72.5 eV (Pt4$f_{7/2}$) indicating the presence of oxidized Pt (*12*) and at 74.5 eV (Pt4$f_{5/2}$) and 71.3 eV (Pt4$f_{7/2}$) following rich conditioning, indicating the presence of Pt° (*12*). Also, shoulders at 76.0 and 72.6 eV following rich conditioning indicate the presence of some oxidized Pt. The observed binding energies for the Pt4*d* peaks are also

TABLE 7

H_2 Uptake Values as Determined from TPR Analysis for a Fresh Pt,Rh/CeO_2 and After *in situ* Rich and Lean Conditioning in the Rich or Lean Synthetic Exhaust Gas Mixture at 450°C for 0.5 hr

Treatment	Peak 1 Temp. range / Max. temp.	Peak 1 (mmole H_2/g)	Peak 2 Temp. range (°C)	Peak 2 (mmole H_2/g)	Peak 3 Temp. range (°C)	Peak 3 (mmole H_2/g)
None (fresh)	30–340 / 180	0.354	340–705	0.076	705–804	0.31
Lean	30–312 / 100	0.303	312–667	0.066	667–805	0.29
Rich	30–235 / 80	0.067	235–703	0.060	703–804	0.30

Note. Pt loading = 0.6 wt%; Rh loading = 0.1 wt%.

TABLE 8

XPS Analysis of the Pt and Rh Oxidation States for Fresh Pt,Rh, 6 wt% Ce/γ-Al_2O_3 and Pt,Rh/CeO_2 Samples and After *in situ* Rich and Lean Conditioning in the Synthetic Exhaust Gas Mixture

Sample	Pretreatment	Peak assignment/position (eV)						Peak Ratios	
		Pt4$f_{7/2}$	Pt4$f_{5/2}$	Pt4$d_{5/2}$	Pt4$d_{3/2}$	Rh3$d_{5/2}$	Rh3$d_{3/2}$	Pt/Ce	Rh/Ce
Pt,Rh, 6 wt% Ce/γ-Al_2O_3[a]	Calcined	—	—	316.8	—	310.3	315.0	0.074	0.053
	Lean	—	—	317.0	—	309.9	314.7	0.034	0.069
	Rich	—	—	315.5	—	308.0	312.8	0.037	0.062
Pt,Rh/CeO_2[b]	Lean	72.5	75.8	315.7	—	—	—	—	—
	Rich	71.3	74.5	314.2	—	—	—	—	—
		72.6	76.0	316.5	—	—	—	—	—

[a] Pt loading (nominal) = 0.6 wt%; Rh loading (nominal) = 0.2 wt%.
[b] Pt loading (nominal) = 0.6 wt%; Rh loading (nominal) = 0.1 wt%.

given in Table 8. The peak locations are consistent with oxidized Pt following lean conditioning and Pt° following rich treatment. Pt° peaks are expected at 314–315.5 eV whereas for oxidized Pt, the Pt4$d_{5/2}$ peak occurs above 315.5 eV (*13*). Rh was not detected by XPS in these samples.

Results for the fresh Pt,Rh,Ce/γ-Al_2O_3 sample and after exposure to the rich and lean gas are also summarized in Table 8. For this sample the Pt loading was 0.6 wt% and the Rh loading was 0.2 wt%. The approximate CeO_2 crystallite size was 60 Å. Again, evidence for oxidized Pt in the fresh and lean conditioned samples is provided by Pt4$d_{5/2}$ peaks located at 316.8 and 317.0 eV, respectively. Following rich conditioning, evidence for Pt° is shown by a Pt4$d_{5/2}$ peak at 315.5 eV. In this sample, Rh was also detected. Like Pt, it is oxidized in the fresh and lean treated samples. This is supported by peaks at 310.3 eV (Rh3$d_{5/2}$) for the fresh sample and at 309.9 eV for the lean treated sample (*13*). Following rich treatment, Rh was found as reduced Rh with peaks at 308.0 eV (*13*). The Pt/Ce and Rh/Ce peak ratios were also measured, and reveal a decrease in the Pt/Ce ratio but no change in the Rh/Ce ratio following gas treatments. Assuming no change in CeO_2 dispersion which is supported by extensive STEM analysis, this indicates partial Pt sintering during the rich and lean treatments while Rh remains highly dispersed.

DISCUSSION

We have found that catalysts formulated with CeO_2 are very sensitive to their exhaust gas environment and can undergo facile activation in a rich gas. The key components responsible for activation are Pt and CeO_2. This is shown clearly by comparing Rise-1 and Rise-2 activities in Table 5 for Pt/CeO_2 and Pt/γ-Al_2O_3. We see that the Pt/CeO_2 catalyst is less active during Rise-1 than Pt/γ-Al_2O_3, whereas after activation the opposite is true. The light-off temperature for CO oxidation decreases 37°C over Pt/γ-Al_2O_3 between Rise-1 and Rise-2, while over Pt/CeO_2, the change is 250°C. Similar results were observed with SO_2, where, after activation, the Pt/CeO_2 catalyst shows light-off advantages of 267°C for CO, 170°C for HC, and 178°C for NO conversion over Pt/γ-Al_2O_3. This demonstrates that Pt–CeO_2 interaction leads to far more effective catalysts than simple Pt/γ-Al_2O_3 after exposure to rich or stoichiometric conditions.

Activation of the catalyst is also very easy. This is shown clearly in Fig. 2 where full activation of the catalyst was shown to occur during the rich drop after a lean hold at 450°C for 0.5 hr. During the rich drop the

catalyst is exposed to 0.26 vol% H_2 for a very short period of time. Figure 2 also shows that these catalysts can exhibit varying activity depending on their immediate exhaust gas history. Activation is also highly reversible as shown in Fig. 3 for testing under SO_2-free conditions and for testing in the presence of SO_2 as shown in Table 3. One significant difference between the SO_2-free tests and tests in the presence of SO_2 was the large detrimental effect of lean conditioning on the fresh catalyst. Lean conditioning was much less detrimental on rich treated samples, as seen from a comparison of the results in Fig. 5 and Table 3. It is hypothesized that the large detrimental effect of lean conditioning on the performance of the fresh catalyst as compared to the rich treated sample may have been due to different degrees of NM sintering before the lean treatment. After the rich treatment the NMs are expected to be more sintered and thus less likely to undergo complete reoxidation as a result of the lean conditioning.

Both the effect of CeO_2 crystallite size on activity and the physicochemical properties of the catalysts suggest that Pt selectively migrates to CeO_2 during catalyst preparation. Thus, the CeO_2 crystallite size effect reflects increasing Pt/Ce interaction with its subsequent improvement in catalyst performance. Direct evidence for this hypothesis comes from STEM studies where Pt was found to be selectively associated with the CeO_2, even though most of the catalyst surface area is γ-Al_2O_3. Indirect evidence comes from noting that performance features of the Pt/CeO_2 catalyst are most similar to the $Pt,Rh,Ce/\gamma$-Al_2O_3 samples having the smallest CeO_2 crystallite sizes. This is clearly seen by comparing performance results for Pt/CeO_2 in Table 5 with the activity results in Figs. 6 and 7. We see the same activation features in catalyst performance as observed for Pt/CeO_2. Further evidence for extensive Pt/Ce interaction comes from the TPR studies outlined in Figs. 8 and 9. Figure 8 indicates that direct Pt/Ce interaction leads to a synergistic reduction of Pt and surface Ce. This synergistic reduction was shown to be a function of CeO_2 crystallite size in Fig. 9 and to be very extensive for samples having small CeO_2 sizes in Figs. 8 and 9.

The results from the present work suggest that CeO_2 is not an inert support but instead undergoes physicochemical changes similar to the NM and that these changes relate to the catalyst's achieving its optimum active state. These changes include reduction of the NM as observed by TPR and XPS and surface Ce reduction as suggested by TPR. NM and Ce reduction is coupled and appears related to the light-off performance of the catalyst after activation. This is supported by a comparison of Figs. 7 and 9. The exhaust gas component responsible for bringing about catalyst activation is H_2, which is present in low levels in the exhaust gas. These correlations suggest that NM in contact with reduced Ce plays a key role in catalyst performance and may represent the most active state of the catalyst.

Direct evidence for the nature of the catalyst's active state comes from TPR and, to a lesser extent, from the XPS studies. The XPS results in Table 8 indicate that the NM in fresh and lean conditioned catalysts is in oxidized states. Rich conditioning clearly leads to reduction of the NM. Since both fresh and lean conditioned catalysts exhibit low activity while rich conditioned catalysts have high activity, it appears that fully reduced NM results in the most active state of the catalyst. Evidence for reduced Ce was not found by XPS of the rich treated samples. This may have been due to partial reoxidation of the catalyst during sample handling or to insufficiently reduced Ce for detection by XPS. The XPS peaks of Ce^{3+} tend to overlap with those of Ce^{4+} (*13, 14*). Evidence for easy reoxidation of Ce^{3+} in the N_2 used for sample handling was obtained from *in situ* reduction experiments in the XPS instrument. Clear evidence for Ce^{3+} could be obtained in the $Pt,Rh/CeO_2$ sample following reduction at 300°C in 1 Torr of H_2. However, exposure of the reduced sample

to the glove box N_2 for 2 days at room temperature led to complete loss of Ce^{3+} features (O_2 concentration was found to be much greater than the 50 ppm values present during sample handling in the TPR). Since the XPS sample handling was done in N_2 having higher O_2 contents than for the TPR experiment, reoxidation of the reduced Ce could easily occur in preparation for the XPS measurement.

The TPR results provide further evidence for the nature of the catalyst's active state. TPR results in Fig. 8 show that Ce not only promotes reduction of the NM but also undergoes a synergistic reduction with the NM. The fraction of CeO_2 that couples with the NM reduction seems to be selectively the surface Ce component. This is supported by (i) the disappearance of the peaks assigned to surface Ce reduction when the NM are present; (ii) direct evidence for reduced Ce observed by XPS following reduction at 300°C; and (iii) thermodynamic unfavorability of bulk Ce reduction at the low temperatures observed for synergistic reductions (*15*). A number of authors have reported H_2 uptake by CeO_2 (*16*), where H_2 consumption was not necessarily associated with Ce reduction. However, the evidence here favors surface Ce reduction as the source of H_2 uptake in TPR. It was further found that decreasing the CeO_2 size led to greater coupling of NM/Ce reduction, as shown in Fig. 9.

The TPR studies of the Pt,Rh/CeO_2 before and after treatment in the exhaust gas give further insight into the nature of the NM/Ce interaction and its relation to the active state of the catalyst. For the fresh and lean conditioned catalyst we again clearly see evidence for synergistic reduction of the Pt and Ce. This is supported by the volume of hydrogen uptake in the low temperature reduction peak, as shown in Table 7, and the absence of surface Ce reduction peaks below 500°C, as reported by other authors (*3, 11*). After lean conditioning, less H_2 is consumed than by the fresh sample, along with a shift to lower temperature. A similar temperature shift is observed for the rich treated sample. The shift to lower temperature indicates easier reduction after exhaust gas treatment. This may be explained by partial noble metal sintering in addition to removal of residual chloride. Sintering is supported by lower Pt/Ce XPS ratios in the Pt,Rh,6%Ce/γ-Al_2O_3 sample following rich and lean conditioning than observed in fresh sample. It has been reported that reduction of partially sintered Pt is easier than reduction of highly dispersed Pt (*17*). The lower H_2 uptake following lean gas treatment may be due to a combination of less Pt reduction and poorer coupling with CeO_2 resulting from partial sintering. Growth of 40–50 Å diameter Pt crystallites is observed in STEM analysis under our testing conditions. When exposed to oxidizing conditions, particles of this size will not fully reoxidize, leaving a substantial fraction of the Pt in the metallic state. Further, as Pt crystallites grow, partial segregation of Pt from its contact with CeO_2 is anticipated. In contrast, the rich conditioned sample showed much lower H_2 uptake indicating that considerable reduction of the catalyst had occurred. The small H_2 uptake by the rich conditioned sample may have been due to reduction of surface "PtO" species and incompletely reduced surface Ce. These observations suggest that the most active state of the catalyst after rich conditioning is reduced noble metal in contact with partially reduced CeO_2.

This study shows that direct interaction between CeO_2 and Pt leads to dramatic improvements in catalyst light-off activity. Since catalyst performance was measured under stoichiometric nonoscillating conditions, the impact of CeO_2 cannot be explained by oxygen storage. Further explanations such as promotion of the water gas shift reaction, promotion of NM dispersion, or stabilization of the support cannot explain the large beneficial effect of CeO_2 under the present testing conditions.

An interesting feature of CeO_2 promotion is the enhanced conversion of all the exhaust

gas components. Also, fresh catalysts show exception CO light-off activity after activation. This is clearly seen by comparing Figs. 6 and 7 and from the data presented in Table 5. Further, CO light-off is promoted to a greater extent than HC or NO light-off, especially in tests without SO_2, as seen by comparing light-off temperatures in Figs. 6 and 7 and Table 5. Since CO can inhibit oxidation reactions over reduced Pt and Rh, the removal of CO via its effective oxidation at low temperatures may lead to more effective HC conversion.

In summary, our results indicate that the most active state of the catalyst is reduced surface Ce in contact with reduced NM which is particularly effective in CO oxidation. These conclusions are in general agreement with the proposals of Sass *et al.* (*8*) and Oh *et al.* (*7*) where the impact of CeO_2 was on CO oxidation. For testing under more severe conditions, such as high temperature and in oscillating rich/lean exhaust gas mixtures, other factors, such as water-gas shift promotion or oxygen storage, may become important in catalyst performance.

ACKNOWLEDGMENTS

The authors are indebted to their respective organizations for financial support, encouragement, and provision of facilities. We acknowledge the assistance of the following colleagues at both Allied–Signal and UOP: Mark T. West for catalyst testing; David E. Mackowiak for catalyst preparation; Jeffry T. Donner and Sharon G. Varga for XPS analysis; Mary A. Vanek and Judy A. Triphahn for XRD analysis; and Tomatsu Imai for helpful discussions and encouragement.

REFERENCES

1. Gandhi, H. S., Piken, A. G., Shelef, M., and Delosh, R. G., SAE Paper No. 760201 (1976).
2. Su, E. C., Montreuil, C. N., and Rothchild, W. G., *Appl. Catal.* **17,** 75 (1985).
3. Harrison, B., Diwell, A. F. and Hallett, C., *Platinum Met. Rev.* **32,** 73, (1988).
4. Kim, G., *Ind. Eng. Chem. Prod. Res. Dev.* **21,** 267 (1982).
5. Sergeys, F. J., Masellei, J. M., and Ernest, M. V., W. R. Grace Co., U.S. Patent 3,903,020 (1974); Hindin S. G., Engelhard Mineral and Chemical Co., U.S. Patent 3,870,455 (1973).
6. Yao, Y. Y.-F., *J. Catal.* **87,** 152 (1984).
7. Oh, S. H., and Eickel, C. C., *J. Catal.* **112,** 543 (1988).
8. Sass, A. S., Shvets, V. A., Savel'era, G. A., Povova, N. M., and Kazanskii, V. B., *Kinet. Katal.* **27,** 894 (1986).
9. Tarasov, A. L., Przheval'skaya, Shvets, V. A., and Kazanskii, V. B., *Kinet. Katal.* **29,** 1181 (1988).
10. Yao, H. C., and Yao, Y. Y.-F., *J. Catal.* **86,** 254 (1984).
11. Johnson, M. F. L., and Mooi, J., *J. Catal.* **103,** 502 (1987).
12. Kim, K. S., Wingrad, N., and Davis, R. E., *J. Am. Chem. Soc.* **93,** 6296 (1971).
13. Muilenberg, G. E., Ed., "Handbook of X-Ray Photoelectron Spectroscopy." Perkin-Elmer Corp., Eden Prairie, MN (1979).
14. Shyu, J. Z., Weber, W. H., and Gandhi, H. S., *J. Phys. Chem.* **92,** 4964 (1988).
15. Bevan, D. J. M., *J. Inorg. Nucl. Chem.* **1,** 49 (1955).
16. Fierro, J. L. G., Soria, J., Sanz, J., and Rojo, J. M., *J. Catal.* **66,** 154 (1987).
17. McCabe, R. W., Wong, C., and Woo, H. S., *J. Catal.* **114,** 354 (1988).